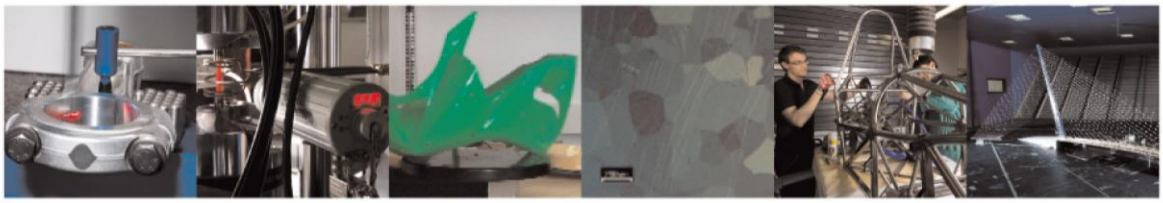

Global sensitivity analyses of a selective laser melting finite element model: influential parameters identification

Bruna-Rosso, Claire; Demir, Ali Gökhan; Vedani, Maurizio; Previtali, Barbara

This is a post-peer-review, pre-copyedit version of an article published in NTERNATIONAL JOURNAL OF ADVANCED MANUFACTURING TECHNOLOGY. The final authenticated version is available online at: http://dx.doi.org/10.1007/s00170-018-2531-7

DIPARTIMENTO DI MECCANICA ■ POLITECNICO DI MILANO
via G. La Masa, 1 ■ 20156 Milano ■ EMAIL (PEC): pecmecc@cert.polimi.it
http://www.mecc.polimi.it
Rev. 0

The International Journal of Advanced Manufacturing Technology manuscript No.
(will be inserted by the editor)

Global Sensitivity Analyses of a Selective Laser Melting Finite Element Model: Influential Parameters Identification

Claire Bruna-Rosso · Ali Gökhan Demir · Maurizio Vedani · Barbara Previtali

Received: date / Accepted: date

Abstract Selective laser melting, an additive manufacturing technique that allows 3D printing of metal components, has recently gained great interest. Despite its growing popularity, this technology continues to suffer from deficiencies in standards and qualifications, factors that limit wide industrial use. Numerical modeling is currently a standard tool in production engineering for both process optimization and a more comprehensive understanding of the process physics. However, inherent to any model implementation and computation are various sources of uncertainties and errors. It is of major importance to identify them and assess whether their influences on outputs is significant. This can be accomplished using sensitivity analysis. To determine the parameters that most influence variability in the computational results, global sensitivity analyses were performed using an in-house developed nonlinear finite element model of the selective laser melting process. The computational load was limited by utilizing a 2D model for a single-layer simulation. The studies were performed on 26 process parameters including material properties, their dependencies on temperature, laser-related parameters, and boundary conditions, among others. Computed maximal temperatures and melt pool widths and lengths were obtained. Two sensitivity analyses were performed using the elementary effect method: one included process parameters and the other excluded them. Among the 26 input parameters tested, 16 did not show significant effects in either study. By including process parameters, they were found to be the most influential. By excluding them, the significant influence of the emissivity coefficient on output variability was revealed. These results evidence the parameters that should be given higher priority in modeling, the sources of error to be considered during validation, and insights into which parameters should be prioritized for further studies, both experimental and computational.

Keywords Selective laser melting · Finite elements · Simulation · Global sensitivity analysis

Dipartimento di Meccanica, Politecnico di Milano, Via la Masa 1, 20156 Milan, Italy
E-mail: claire.brunarosso@polimi.it

Nomenclature

α	Power absorption
ε	Surface emittance
ϕ	Nodal FEM powder fraction
ϕ_{pow}	Powder porosity
ρ_{l_0}	Constant of the liquid metal density model [$\mathrm{kg\,m^{-3}}$]
ρ_{l_1}	First order coefficient of the liquid metal density model [$\mathrm{kg\,m^{-3}\,K^{-1}}$]

ρ_{s_0}	Constant of the solid metal density model [$\mathrm{kg\,m^{-3}}$]
ρ_{s_1}	First order coefficient of the solid metal density model [$\mathrm{kg\,m^{-3}\,K^{-1}}$]
σ	Stefan-Boltzmann constant
φ	Nodal FEM phase fraction
a_{front}	Goldak heat source parameter [µm]
a_{rear}	Goldak heat source parameter [µm]
c	Goldak heat source parameter [µm]
c_0	Constant of the heat capacity model [$\mathrm{J\,kg^{-1}\,K^{-1}}$]
c_1	First order coefficient of the heat capacity model [$\mathrm{J\,kg^{-1}\,K^{-2}}$]
c_2	Second order coefficient of the heat capacity model [$\mathrm{J\,kg^{-1}\,K^{-3}}$]
D_{pow}	Powder diameter [µm]
h	Convection coefficient [$\mathrm{W\,m^{-2}\,K}$]
h_{PB}	Layer thickness [µm]
k_0	Constant of the thermal conductivity model [$\mathrm{W\,m^{-1}\,K^{-1}}$]
k_1	First order coefficient of the thermal conductivity model [$\mathrm{W\,m^{-1}\,K^{-2}}$]
k_{bulk}	Thermal conductivity of the bulk AISI316L stainless steel [$\mathrm{W\,m^{-1}\,K^{-1}}$]
k_g	Interstitial gas heat conductivity [$\mathrm{W\,m^{-1}\,K^{-1}}$]
k_R	Thermal conductivity of the powder bed resulting from radiation [$\mathrm{W\,m^{-1}\,K^{-1}}$]
L	Latent heat of phase change [$\mathrm{kJ\,kg^{-1}}$]
P	Laser power [W]
Q	Laser heat input density [$\mathrm{W\,m^{-3}}$]
T_L	Liquidus temperature [K]
T_S	Solidus temperature [K]
T_{amb}	Ambient temperature [K]
T_{sint}	Sintering temperature [K]
v	Laser displacement speed [$\mathrm{mm\,s^{-1}}$]
μ_i	Mean of EE_i over the r starting points
σ_i	Standard deviation of EE_i over the r starting points
EE_i^j	Elementary effect of parameter i at starting point j
r	Number of starting point in the sensitivity analyses
SEM_i	Standard error of the mean of parameter i

1 Introduction

Selective laser melting (SLM) is a layer-based additive manufacturing processes. It allows building functional products layer by layer to obtain a final 3D geometry. Owing to the high energy input provided by the laser, a variety of materials, including metals, are eligible to this process. This technique allows building a large range of geometries, leading to a wide design freedom and flexibility. This makes it especially appealing for applications in the aerospace and biomedical fields. However, many unknowns continue to surround this process. The laser processing of metal powder layers is complex and involves numerous physical phenomena of various types and time and space scales. Figure 1 illustrates the process and summarizes its major physical phenomena. Current knowledge about SLM does not allow its complete and stable management. The process is quite often not qualified, few standards have been set, and those that have are for a reduced range of applications, limiting its industrial development [1]. To improve knowledge about a process, design of experiment techniques can be used ([2,3]). However characterizing a process by the mean of experimental investigations could prove to be costly, and the experimental region where parameters can be chosen is limited and difficult to extend. Developing a realistic model of the process and gaining insight through simulations could address the issue of flexibility[4]. Nevertheless, because the process is intrinsically multi-physic and multi-scale, realistic modeling from both the physic and geometrical points of view is computationally heavy [5]. Consequently, characterizing the process and exploring its large input space can also prove to be challenging from a computational point of view. Moreover, numerical models are deterministic and the large majority of the published models do not account for the uncertainties surrounding all the input parameters. This is why alternative approaches involving statistical methods together with reduced and simple models have been developed. A comprehensive list of uncertainty sources in the SLM models can be found elsewhere [6] where the issue of uncertainty quantification in SLM simulation is tackled using a low-order model. Hu & Mahadevan made an extensive discussion on the utilization of uncertainty quantification and management methods in additive manufacturing and illus-

trated their application to laser nanoparticle sintering [7]. Kamath [8] used an iterative procedure that combine data mining with statistical inference to couple results from simulations with those from experiments. It allowed development of surrogate models which were then used, among others, to perform uncertainty quantification analyses. However the major sources of uncertainty remain unknown, but perhaps can be identified by performing a sensitivity analysis as seen in Asserin et al. [9] on a welding process Finite Element Model (FEM). Indeed, as Saltelli et al [10] introduce it, it is "The study of how uncertainty in the output of a model (numerical or otherwise) can be apportioned to different sources of uncertainty in the model input". Performing such an analysis allows to identify those "sources of uncertainty" whose better knowledge and management would improve the most the accuracy of the FEM results. Those authors also explained that "law-driven models tend to be overparametrized", meaning that some variables included in the model because they appear in the equations being solved do not have a relevant effect on the outputs. A better understanding of the influential variables on the FEM results would orientate future studies toward an improved experimental characterization and modeling of those parameters only. This allows to limit the effort spent in experiments to accurately determine or measure unknown input parameters to the ones that have a significant impact on the model outputs. Together with the definition of the parameters that are responsible of the main part of the output uncertainty, the sensitivity analysis also helps to reduce subsequent computational experiment campaigns by limiting their variables only to the factors with significant effects, all the others being fixed to their mean. Criales et al. [11] performed a local sensitivity analysis on a FEM of Inconel selective laser melting. They used a perturbation method consisting in varying of a small amount (10%) each parameter from their nominal value. While being computationally cheap, this method has the disadvantage of producing information only at a local level [12]. However, some of the parameters entering the SLM finite element model may vary significantly. For instance the emissivity of stainless steels may fluctuate between 0.1 and 0.8 depending on the material state, temperature, oxidation level etc [13], highlighting the need for a study on a wider range of parameter values. Therefore, we propose a global sensitivity analysis (GSA) based on a reduced SLM finite element model.

2 Finite Element Model

The model under study is an in-house developed FEM implemented using the deal.ii library [14]. A more comprehensive description of the model can be found elsewhere [15]. The material used is the 316 stainless steel.

2.1 Mathematical Formulation

The current model aims to simulate layer-based additive manufacturing of metal. The main features that must be taken into account are :

- A moving heat source (provided by a laser beam)
- Convective cooling and radiation between the free surfaces of the part and the building chamber atmosphere
- Temperature- and phase-dependent material properties

Those characteristics translate into the following partial differential equation system:

$$\begin{cases} c_p(T)\rho(T)\frac{\partial T(\mathbf{x},t)}{\partial t} - \nabla.k(T)\nabla T(\mathbf{x},t) = f(\mathbf{x},t) & \text{in } \Omega, \text{t} > 0 \\ T(\mathbf{x},t) = T_{\text{amb}} & \text{in } \Omega, \text{t} = 0 \\ T(\mathbf{x},t) = T_{\text{amb}} & \text{on } \Gamma_D, \text{t} > 0 \\ k(T)\frac{\partial T(\mathbf{x},t)}{\partial n} = \alpha(T) & \text{on } \Gamma_R, \text{t} > 0 \end{cases} \quad (1)$$

With :

$$\begin{aligned} \rho &= \rho(T, \Phi) \\ c_p &= c_p(T, \Phi) \\ k &= k(T, \Phi) \\ \alpha(T) &= \sigma\varepsilon(T^4 - T_{\text{amb}}^4) + h(T - T_{\text{amb}}) \end{aligned}$$

Where T is the temperature, Φ is the fraction of powder/consolidated (solid or liquid) material, ρ is the density, k is the thermal conductivity, c_p is the thermal capacity, T_{amb} is the ambient temperature in the building chamber, h is the convection coefficient, ε is the material emissivity, σ is

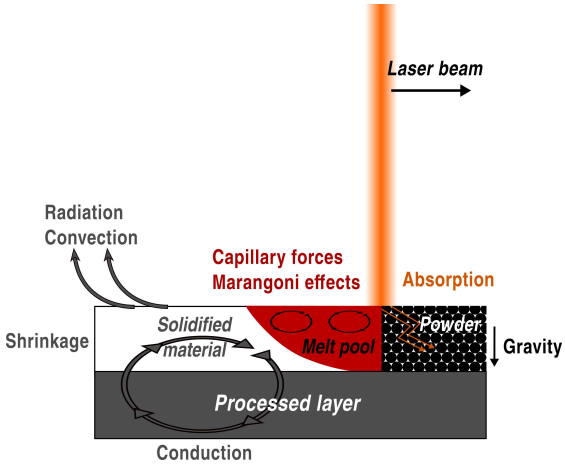

Fig. 1 The selective laser melting process and major physical phenomena

the Stefan-Boltzmann constant, Γ_D is the contact area with the substrate, Γ_R is the contact area with the environing gas and $f(\mathbf{x},t)$ is the heat input provided by the laser (see subsection 2.2) and the phase change.

2.2 Laser Modeling

The laser heat source has been implemented using the Goldak [16] model, as previously done in SLM modeling [17,18]

$$\begin{aligned} Q &= \frac{6\sqrt{3}P\alpha}{a_{\text{front}}bc\pi\sqrt{\pi}}\exp[-(\frac{3x^2}{a_{\text{front}}^2}+\frac{3y^2}{b^2}+\frac{3z^2}{c^2})] \text{ if x>0} \\ Q &= \frac{6\sqrt{3}P\alpha}{a_{\text{rear}}bc\pi\sqrt{\pi}}\exp[-(\frac{3x^2}{a_{\text{rear}}^2}+\frac{3y^2}{b^2}+\frac{3z^2}{c^2})] \quad \text{if x<0} \end{aligned} \tag{2}$$

Where x, y and z are the coordinates of the center of the moving laser (i.e. with the origin is at the center of the beam) a_{rear}, a_{front}, b and c are the geometric parameters of the rear and front quadrant, respectively, of the double ellipsoid heat source, P is total laser power and α is the absorption efficiency.

2.3 Material Properties

2.3.1 Density ρ

The density ρ is computed according to the experimentally based model of Mills [19]. It takes into account the influence of three variables: the temperature T, the powder fraction ϕ, and the phase fraction φ.
$\phi = 1$ if at the point considered, the material is all powder, $\phi = 0$ if it is all consolidated.
$\varphi = 1$ if at the point considered, the material is all solid, $\varphi = 0$ if it is all liquid.

$$\begin{aligned} \rho_s &= \rho_{s_0} - \rho_{s_1}(T - 298.15) \\ \rho_l &= \rho_{l_0} - \rho_{l_1}(T - 1723.15) \\ \rho &= \rho_l(1-\varphi)(1-\phi) + \rho_s\left[\phi_{\text{pow}}\phi + (1-\phi)\varphi\right] \end{aligned} \tag{3}$$

Where :
ρ_s: solid temperature dependent density
ρ_l: liquid temperature dependent density
ϕ_{pow} : powder bed porosity ($\simeq$ 0.4 for a randomly packed powder bed)

2.3.2 Emissivity ε

The model, whose full derivation can be found elsewhere [20], account for the particle packing, size, and the influence of interstitial spaces. It leads to the following formulae:

$$\varepsilon_{\text{pow}} = A_H\varepsilon_H + (1-A_H)\varepsilon_S \text{ with:} \tag{4}$$

$$A_H = \frac{0.908\phi_{\text{pow}}^2}{1.908\phi_{\text{pow}}^2 - 2\phi_{\text{pow}} + 1}$$

$$\varepsilon_H = \frac{\varepsilon_S[2 + 3.082(\frac{1-\phi_{\text{pow}}}{\phi_{\text{pow}}})^2]}{\varepsilon_S[1 + 3.082(\frac{1-\phi_{\text{pow}}}{\phi_{\text{pow}}})^2] + 1}$$

where ε_S is the emissivity of the solid and ε_H the emissivity of the spaces.

2.3.3 Heat capacity c_p

Heat capacity varies with temperature. The model is a second order polynomial regression obtain from experimental data [21].

$$c_p(T) = \begin{cases} c_0 + c_1\,T - c_2\,T^2, & \text{for } T \le T_{\text{sint}} \\ 603.9, & \text{for } T > T_{\text{sint}} \end{cases} \quad (5)$$

where T_{sint} is the sintering temperature of the material.

2.3.4 Heat conductivity

Heat conductivity is dependent on both temperature and the powder fraction. One model is used for the bulk material, and another for the powder. The two are then combined using the law of mixtures:

$$k = \phi\,k_{\text{pow}} + (1-\phi)\,k_{\text{bulk}} \quad (6)$$

Powder heat conductivity As derived by Sih & Barlow [20], powder heat conductivity is:Second analysis

$$\begin{aligned} k_{\text{pow}} = k_g \Big\{ & (1-\sqrt{1-\varphi}(1-\frac{\phi_{\text{pow}} k_R}{k_g}) \\ & + \sqrt{2-\phi_{\text{pow}}}\Big[\frac{2}{(1-\frac{Bk_g}{k_s})^2}\log\frac{k_s}{Bk_g} \\ & - \frac{B+1}{2} - \frac{B-1}{1-\frac{Bk_g}{k_s}}) + \frac{k_R}{k_g}\Big]\Big\} \end{aligned} \quad (7)$$

Where k_{pow} is the effective thermal conductivity of the powder bed, k_g is the thermal conductivity of the gas phase, k_s is the thermal conductivity of the solid phase, and k_R is the thermal conductivity of the powder bed resulting from radiation. The last of these variables is represented by:

$$k_R = \frac{4\varepsilon\sigma T^3 x_R}{1 - 0.132\varepsilon}$$

ε = powder bed emissivity calculated using equation 4, σ is the Stefan-Boltzmann constant and x_R is the powder particle diameter.

Bulk material heat conductivity The model is temperature-dependent and is a regression computed from experimental data [21].

$$k_{\text{bulk}} = \begin{cases} k_0 + k_1\,T, & \text{for } T \le T_{\text{sint}} \\ 26.51, & \text{for } T > T_{\text{sint}} \end{cases} \quad (8)$$

3 Global Sensitivity Analysis

The global sensitivity analysis was performed using the workflow recommended by Pianosi et al [12] (see subsection 3.2). The sensitivity indices computations and visualization were completed using the Matlab®toolbox SAFE [22]. The study was performed in two analyses. The first included the process parameters (laser power, laser speed, layer thickness) and the power absorption which are experimentally known to be influential on the process output. This analysis was used to evaluate model adequacy to empirically observed results, and thus verify its physical consistency, and to detect potential interactions between parameters. The second analysis did not include these parameters. The main purpose of this step of the study is to elucidate the effects of the variables that could have been concealed by influences of the most significant parameters in the first study.

3.1 Inputs and Outputs of the GSA

In the FEM, 26 variables were found to potentially influence the computation and thus were used as inputs to the initial GSA. Where possible, the range of values was chosen based on physical considerations, otherwise an interval of $\pm 15\%$ was chosen (see Table 1).

The outputs considered for the GSA were the maximal temperature and the melt pool length and depth, each measured when deemed stable. An illustration of those variables is provided in Fig. 2.

3.2 Sensitivity Analysis Method

After identifying and selecting the relevant inputs and outputs, the right GSA method had to be cho-

Symbol	Description	Variation range	Nature
ε	Surface emittance	0.1 - 0.9	Boundary Condition (BC) Data
h	Convection coefficient	5 - 25 $\mathrm{W\,m^{-2}\,K^{-1}}$	
T_{amb}	Ambient temperature	288 - 298 K	
L	Latent heat of phase change	260 - 285 $\mathrm{kJ\,kg^{-1}}$	Material properties
ρ_{l_0}	Constant of the liquid metal density model	5849 - 7913 $\mathrm{kg\,m^{-3}}$	
ρ_{l_1}	First order coefficient of the liquid metal density model	0.6545 - 0.8855 $\mathrm{kg\,m^{-3}\,K^{-1}}$	
ρ_{s_0}	Constant of the solid metal density model	6757.5 - 9142.5 $\mathrm{kg\,m^{-3}}$	
ρ_{s_1}	First order coefficient of the solid metal density model	0.426 - 0.576 $\mathrm{kg\,m^{-3}\,K^{-1}}$	
c_0	Constant of the heat capacity model	310.6 - 420.2 $\mathrm{J\,kg^{-1}\,K^{-1}}$	
c_1	First order coefficient of the heat capacity model	0.346 - 0.468 $\mathrm{J\,kg^{-1}\,K^{-2}}$	
c_2	Second order coefficient of the heat capacity model	$1.47e^{-4}$ - $1.99e^{-4}$ $\mathrm{J\,kg^{-1}\,K^{-3}}$	
k_0	Constant of the thermal conductivity model	7.66 - 10.36 $\mathrm{W\,m^{-1}\,K^{-1}}$	
k_1	First order coefficient of the thermal conductivity model	$1.3e^{-2}$ - $1.76e^{-2}$ $\mathrm{W\,m^{-1}\,K^{-2}}$	
α	*Power absorption*	0.1 - 0.9	
T_S	Solidus temperature	1638 - 1658 K	
T_L	Liquidus temperature	1663 - 1683 K	
T_{sint}	Sintering temperature	997 - 1349 K	
ϕ_{pow}	Powder porosity	0.2 - 0.8	Powder bed properties
D_{pow}	Powder diameter	10 - 40 µm	
k_g	Interstitial gaz heat conductivity	0.025 - 0.05 $\mathrm{W\,m^{-1}\,K^{-1}}$	
h_{PB}	*Layer thickness*	40 - 60 µm	
a_{front}	Goldak heat source parameter	85 - 115 µm	Laser heat source properties
a_{rear}	Goldak heat source parameter	340 - 460 µm	
c	Goldak heat source parameter	42.5 - 57.5 µm	
P	*Laser power*	50 - 250 W	
v	*Laser displacement speed*	50 - 500 $\mathrm{mm\,s^{-1}}$	

Table 1 Parameters included in the GSA and their domains of variation ([19,20,21]). Parameters in italic were removed for the second study

sen. The objective of the present study was to determine the most influential parameters on the output variability, or how uncertainty in the output(s) can be linked to the input ones. The model is being used in a 2D and geometrically restricted (1.5mm x 1.05mm) configuration to limit the computation time. Each simulation performed on a 8 cores @ 3.60GHz computer required 150s. With this in mind, the goal of the study, and the number of parameters, the most suitable method appeared to be the elementary effect (EE) test. It is the global prolongation of the local method proposed by Criales et al. [11]. It consists in computing the local output variations resulting from input perturbations from various points mapping the entirety of the input feasibility space, instead of just one point corresponding to the nominal value of the parameters. More specifically, this method considers for every starting point $\mathbf{x}^j$ of the analysis (see section 3.3), how much the output varies when the ith parameters is perturbed and all the others remain unchanged. This variation is known as the elementary effect of the parameter x_i. The statistic then used as a sensitivity measure, EE_i is the mean of the elementary effects of the parameter i over the r starting points of the study, and this is computed as:

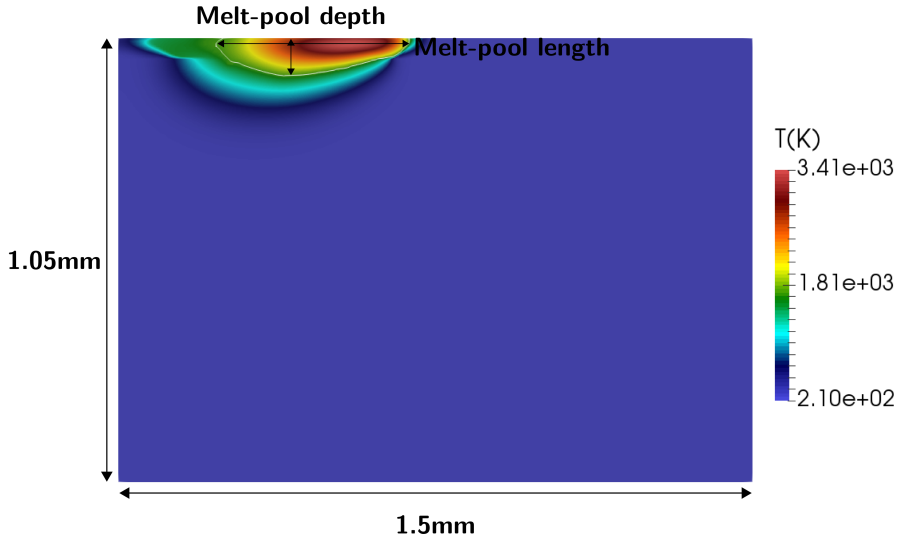

Fig. 2 Output measurements. The white line represents the isothermal $T = T_{\text{liquidus}}$

$$EE_i^j = \frac{g(\mathbf{x}_1^j, ..., \mathbf{x}_i^j + \Delta_i^j, ..., \mathbf{x}_M^j) - g(\mathbf{x}_1^j, ..., \mathbf{x}_i^j, ..., \mathbf{x}_M^j)}{\Delta_i^j} \quad (9)$$

$$\mu_i = \frac{1}{r}\sum_{j=1}^{r} EE_i^j$$

$$\mu_i^* = \frac{1}{r}\sum_{j=1}^{r} |EE_i^j|$$

The variable μ_i^* was preferred because the absolute value prevents quantities from canceling each other out due to their signs.
As explained by Pianosi et al [12], it is common to compute on top of the elementary effect mean its standard deviation (see equation 10). It provides a measure of both the interaction between parameter $\mathbf{x}_i$ and other parameters, and its own non-linear effects.

$$\sigma_i^2 = \frac{1}{r-1}\sum_{j=1}^{r}(EE_i^j - \mu_i)^2 \quad (10)$$

3.3 Sample size and sampling strategy

Sample size N is function of the number of parameters, M, and the number of starting points r: $N = r(M+1)$. M being imposed by the model, only r remains to be fixed. No clear method could be found in the literature, but rather suggestions about how to set it. Increasing the number of starting point reduces the confidence bound around the sensitivity indices and thus increases the reliability of the results. On the other hand, an excessive number of starting points would lead to an unaffordable amount of simulations. In the present study 55 starting points were used leading to 1485 simulations in the first analysis and 1265 in the second one. An *a posteriori* convergence study was performed to check whether the results would have been affected by increasing r.
The sampling strategy consisted in selecting the r starting points inside the input space and the input variations Δ_i. The method called the radial-based design was used here for efficiency purposes (see [23] and the references therein for more details).

4 Results

The EE means and standard deviations are presented in Figs. 3 and 5. The criteria applied to separate the parameters with respect to their influence is similar to the one used elsewhere [24] and are as follows:

- if $\mu_i^* \leq 0.1$: The parameter is not influential.
- if $\mu_i^* > 0.1$ and $\sigma_i \leq$ SEM : The parameter is influential in a linear way.

– if $\mu_i^* > 0.1$ and $\sigma_i >$ SEM : The parameter is influential in a nonlinear way and/or includes interactions.

The standard error of the mean is symbolized as SEM and it is determined as: SEM $= \sigma/\sqrt{r}$

4.1 Analysis including process parameters

4.1.1 Elementary effects' means and standard deviations

The computed elementary effects' means and standard deviations are displayed in Fig. 3. Each output was affected similarly in that two parameters (P and α) were very significant, and a few parameters influenced output variability at a lower level. All other parameters cluster in the non significant area. No parameters had linear effects on outputs; all had either nonlinear effects or interacted with other factors.

4.1.2 Convergence analysis

An *a posteriori* convergence analysis was performed to ensure that the number of starting points was sufficient to obtain stable results. In this study, the EEs computation comprised fewer starting points, and new results were gradually added to recompute them. Above a certain threshold, adding starting points did not significantly influence the EEs, signifying that convergence was attained. The analysis showed that this threshold was reached at $r = 49$.

Figure 4 shows how μ^* changes with r for maximal temperature in the first analysis. The curve shows relative stability when $r \geq 49$ which validates *a posteriori* the number of starting points chosen. For the other two outputs, similar behaviors were observed.

4.2 Analysis exclusing process parameters

Results for the second analysis are shown in Fig. 5. By removing the most influential parameters, it is possible to better distinguish between the others with respect to the first analysis. For the maximal temperature, emissivity was much more influential than all other parameters, which is in accordance with the local sensitivity analysis performed by Criales et al [11]. As in the first study, no parameters showed a linear effect, confirming that all either had nonlinear effect or interacted with other factors.

A summary of all influential parameters on the three outputs after both sensitivity analyses can be found in Table 2.

5 Discussion

The results of the first analysis confirmed one expected behavior of the model. Indeed the model is very sensitive to the laser power and the absorption coefficient. Considering both are directly proportional to the amount of heat provided to the part, and they multiply one another, it is logical that they significantly influence both the mean and standard deviation of output variabilities. Another noticeable result is that laser displacement speed is an influential parameter. This agrees with experimental observations [25]. The identification of the process parameters as significant is also supporting the model physical consistency since it reproduces the action of experimentally identified influential parameters.

The second analysis allowed an additional step in the screening process. In addition to the 4 primary parameters identified in the first step, one was added for the maximal temperature output, two for the melt pool depth output and five for the melt pool length output. In this analysis, the influence of the emissivity coefficient appeared clearly. This is consistent with the physics because it governs the most important cooling phenomenon: radiation. It is also in accordance with a previous study performed on the surface cooling coefficient in additive manufacturing modeling [26]. With very high temperatures inside and around the melt pool, the difference between the atmospheric temperature and that of the material is wide leading to significant thermal transfers. ε is a very difficult parameter to measure, and can vary widely with factors such as

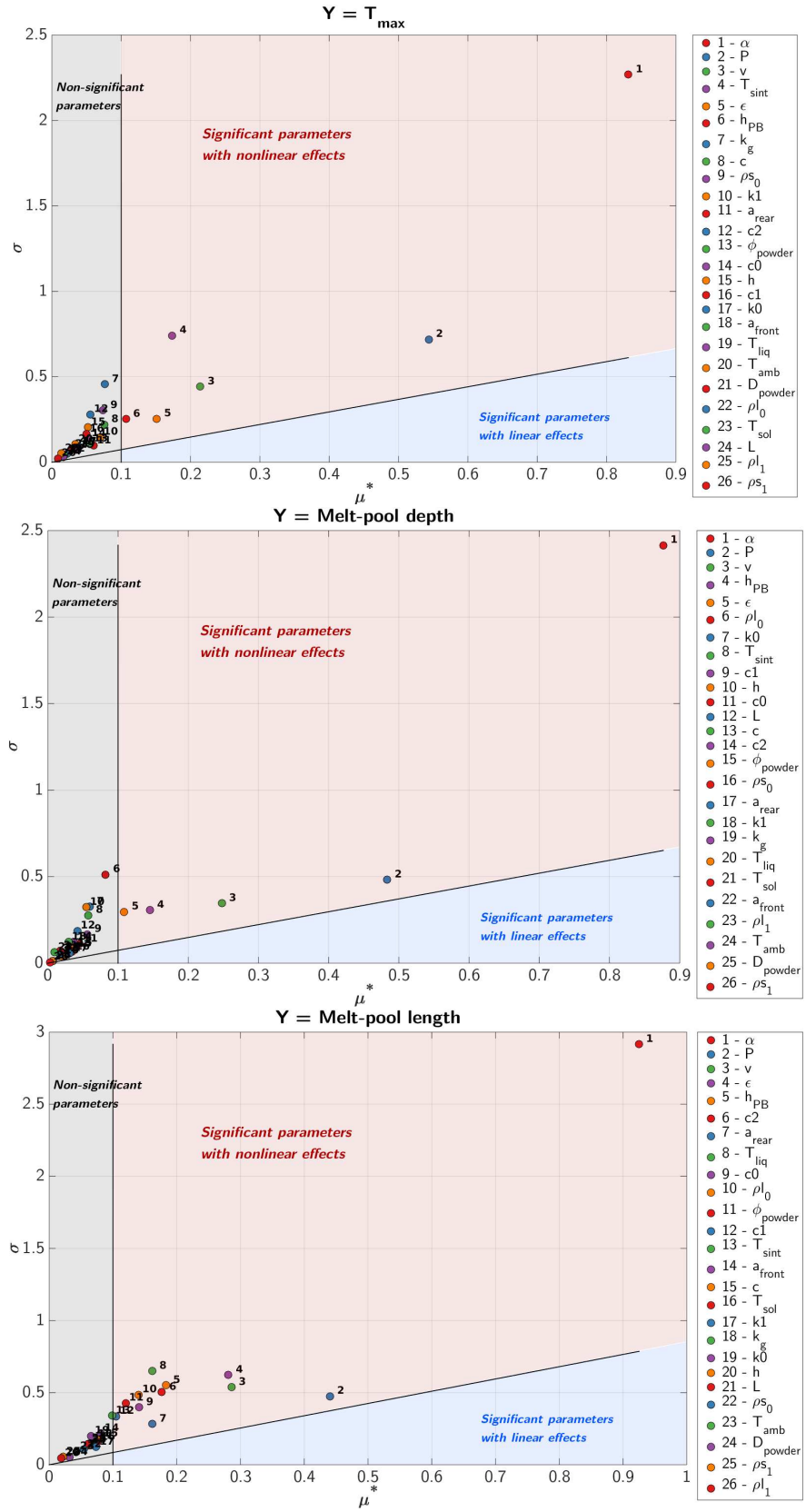

Fig. 3 Means and standard deviations for the elementary effects for three outputs, Analysis 1

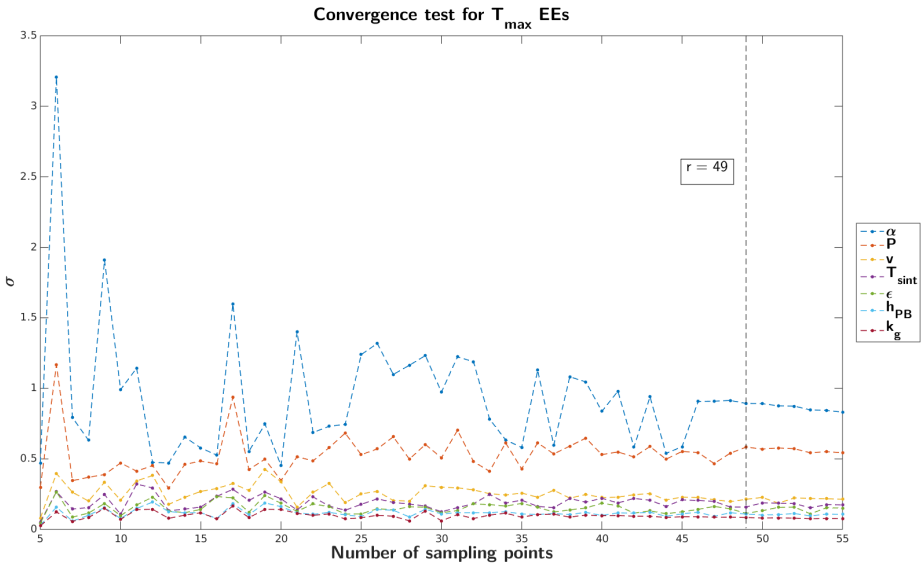

Fig. 4 Convergence study of EEs computation for maximal temperature. For clarity, only the most influential parameters are plotted

Table 2 The influential parameters for the three outputs of interest.

Output	Number of significant parameters	Parameters
Maximal Temperature	5	P, α, v, h_{PB}, ε
Melt pool depth	6	P, α, v, h_{PB}, ε, a_{rear}
Melt pool length	9	P, α, v, h_{PB}, ε, c_1, a_{rear}, k_0, ρ_{s0}

roughness or material state (solid - liquid- powder) which makes it difficult to estimate as well. However the study shows that uncertainty in emissivity impacts outputs, suggesting that more effort should be put in its characterization. Some material property factors also influenced the melt pool length. Because it is parallel to the laser displacement, it is the direction in which thermal conduction is greatest. It is thus not surprising to see that factors included in the conductivity, heat capacity and density functions (see Eqs. 5, 4, 6) influenced the melt pool length. Indeed those material properties directly affect the kinetics of thermal conduction.

Moreover, it was visible in both studies that, except in a few cases, variability in a parameter had a low level of influence on outputs. Thus, the current model is robust with respect to most of the non-controllable and non-measurable input variabilities which will always exist in the properties of elements such as materials or powders. Both studies led to the conclusion that no parameter had a linear influence; therefore, all parameters either interacted or had nonlinear effects. This can be explained in several ways. First, the model is fully nonlinear. The greatest nonlinearities were close to the areas where thermal gradients were sharpest. Because the outputs measured belonged to that area, it is not surprising that elevated EE standard deviations were found. Second, the various equations that govern time and space evolution of temperature (Eq. 1), heat source (Eq. 2), or material properties (Eq. 5, 4, 6) clearly show how all factors included in this study could not act independently. They necessarily are connected to other variables, leading to large standard deviations for elementary

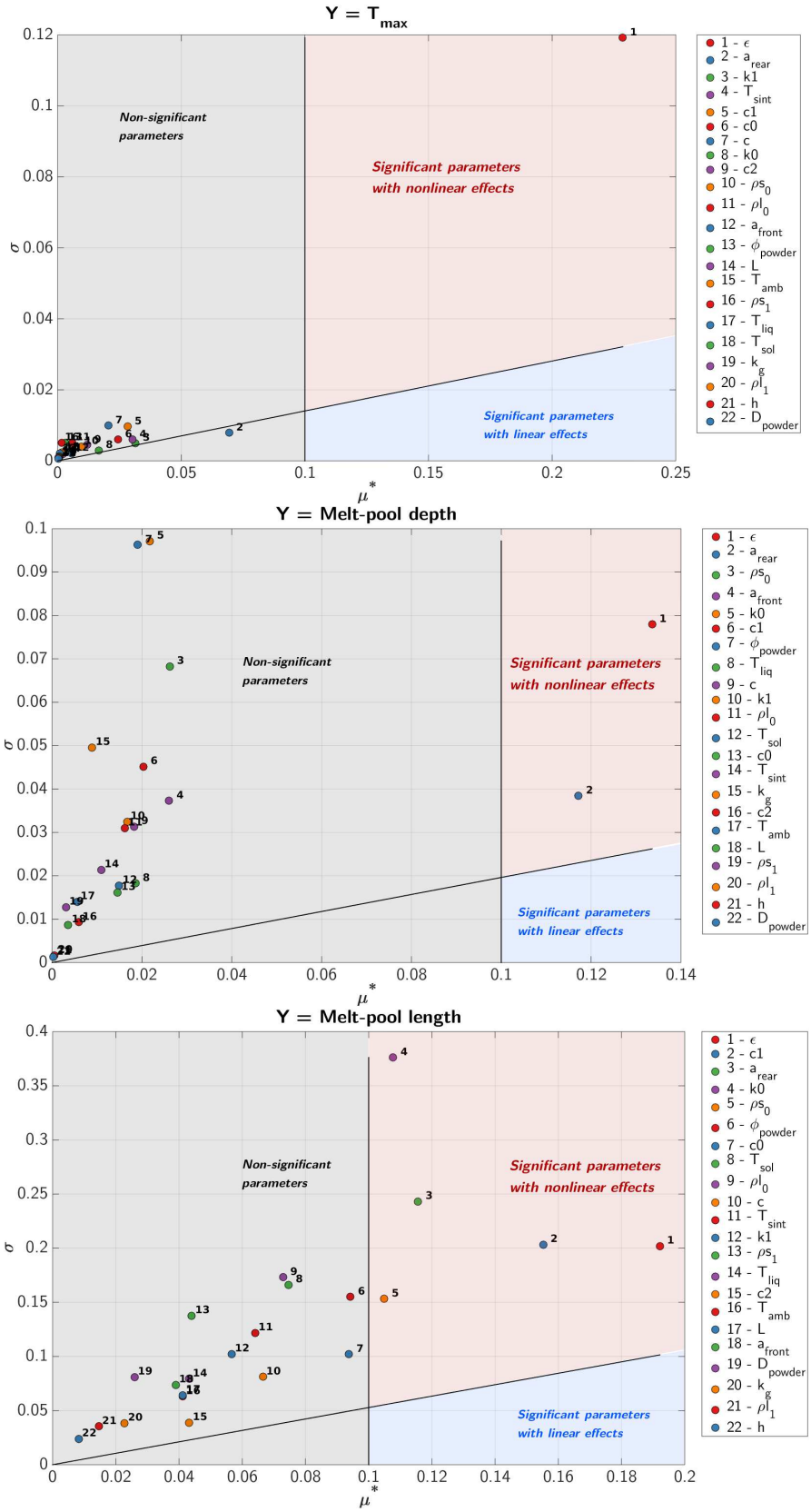

Fig. 5 Means and standard deviations for the elementary effects for the three outputs, Analysis 2

effects.

The simulations comprised for the laser heat input a model which was experimentally calibrated. This model does not include laser beam diameter, although it indirectly acts on parameters a_{rear}, a_{front}, b and c (Eq. 2). Consequently it was not possible to include the laser beam diameter variability in this GSA. However the second study proved that a_{rear} was influential suggesting that laser radius would play a role in output variability in SLM.

The simulations were performed using a single material (AISI316L stainless steel). Considering the large amount of materials processable using SLM, and their discrepancies in terms of thermal behavior [27,28], their sensitivity responses may be different and should be considered for further studies.

These analyses were performed on three specific outputs, deemed to be among the most representative of the process. However they are limited with respect to the amount of data computed. Other output choices might have led to different sensitivity results. Measuring the output in a region close to the laser might magnify laser-related properties, thus minimizing the apparent effects of others. Moreover the model on which the simulations were performed was confined, thus limiting the extension of the results to actual applications. For example, by having a restricted geometry, the effects of boundary condition parameters (e.g, emissivity ε) can be overestimated. Parameters such as the hatching distance, which characterizes the displacements of the laser in the unrepresented dimension, could not be studied.

Up to now, most SLM process models, including the one used in this study, account for power absorption as a simple coefficient which scales the amount of heat actually absorbed by the material. Considering its influence, the absorption phenomenon should be more thoroughly modeled. King et al [5] found that power absorption process was key in the fusion process. Toward more accurate modeling, some efforts should be placed in the characterization of α.

As a screening method, the elementary effect test does not allow parameters to be ranked. Quantitative estimates of their influences on output variability are similarly impossible. Further studies using only the significant parameters identified in this study will be conducted to obtain quantitative results using, for example, variance-based methods [12]. Because of the computational load, those methods could not have been utilized without first reducing the number of parameters by applying a screening step.

6 Conclusion

A novel framework for the global sensitivity analysis of a reduced finite element model of the SLM process of the AISI316L stainless steel was used. The study was divided in two sub-analyses, one including and one excluding the process parameters. Utilizing the elementary effect test, the input parameters that most influence the melt-pool geometry and peak temperature variabilities computed with an in-house developed FEM were identified and analyzed. The first analysis confirmed the physical consistency of the FEM by disclosing the significance of the process parameters P, v and h_{PB} and the power absorptivity α, known as influential. The second analysis, excluding those prominent parameters, revealed the influence of several other parameters (ε, c_1, a_{rear}, k_0 and ρ_{s0}) previously concealed. The limited amount of influential parameters showed the robustness of the present model with respect of the majority of its input variabilities. However, future studies should better-characterize power absorption and emissivity. Indeed, they were found to be highly influential on the FEM output variabilities. A better knowledge and a improved description of those variables would have a significant effect on the deviation of FEM computation with respect to experimental results. Finally, the reduced set of significant parameters obtained from the present could be used in a subsequent GSA using methods that lead to quantitative rather than qualitative results.

Acknowledgements This work was supported by Regione Lombardia (MADE4LO project) under the call “POR FESR 2014-2020 ASSE I - AZIONE I.1.B.1.3.

References

1. W. E. Frazier, "Metal Additive Manufacturing: A Review," *Journal of Materials Engineering and Performance*, vol. 23, no. 6, pp. 1917–1928, 2014.
2. A. G. Demir, P. Colombo, and B. Previtali, "From pulsed to continuous wave emission in SLM with contemporary fiber laser sources: effect of temporal and spatial pulse overlap in part quality," *The International Journal of Advanced Manufacturing Technology*, vol. 91, pp. 2701–2714, Jul 2017.
3. A. G. Demir and B. Previtali, "Investigation of remelting and preheating in SLM of 18Ni300 maraging steel as corrective and preventive measures for porosity reduction," *The International Journal of Advanced Manufacturing Technology*, Jul 2017.
4. M. Markl and C. Körner, "Multiscale modeling of powder bed-based additive manufacturing," *Annual Review of Materials Research*, vol. 46, no. 1, pp. 93–123, 2016.
5. W. E. King, A. T. Anderson, R. M. Ferencz, N. E. Hodge, C. Kamath, S. A. Khairallah, and A. M. Rubenchik, "Laser powder bed fusion additive manufacturing of metals; physics, computational, and materials challenges," *Applied Physics Reviews*, vol. 2, no. 4, 2015.
6. F. Lopez, P. Witherell, and B. Lane, "Identifying uncertainty in laser powder bed fusion additive manufacturing models," *Journal of Mechanical Design*, vol. 138, no. 11, p. 114502, 2016.
7. Z. Hu and S. Mahadevan, "Uncertainty quantification and management in additive manufacturing: current status, needs, and opportunities," *The International Journal of Advanced Manufacturing Technology*, vol. 93, pp. 2855–2874, Nov 2017.
8. C. Kamath, "Data mining and statistical inference in selective laser melting," *The International Journal of Advanced Manufacturing Technology*, vol. 86, no. 5, pp. 1659–1677, 2016.
9. O. Asserin, A. Loredo, M. Petelet, and B. Iooss, "Global sensitivity analysis in welding simulations - What are the material data you really need?," *Finite Elements in Analysis and Design*, vol. 47, no. 9, pp. 1004 – 1016, 2011.
10. A. Saltelli, M. Ratto, T. Andres, J. Cariboni, D. Gatelli, M. Saisana, and S. Tarantola, *Global Sensitivity Analysis: The Primer*. Wiley, 2008.
11. L. E. Criales, Y. M. Arısoy, and T. Özel, "Sensitivity analysis of material and process parameters in finite element modeling of selective laser melting of Inconel 625," *The International Journal of Advanced Manufacturing Technology*, vol. 86, pp. 2653–2666, Oct 2016.
12. F. Pianosi, K. Beven, J. Freer, J. W. Hall, J. Rougier, D. B. Stephenson, and T. Wagener, "Sensitivity analysis of environmental models: A systematic review with practical workflow," *Environmental Modelling & Software*, vol. 79, pp. 214 – 232, 2016.
13. R. H. Bogaard, P. D. Desai, H. H. Li, and C. Y. Ho, "Thermophysical properties of stainless steels," *Thermochimica Acta*, vol. 218, pp. 373 – 393, 1993.
14. W. Bangerth, D. Davydov, T. Heister, L. Heltai, G. Kanschat, M. Kronbichler, M. Maier, B. Turcksin, and D. Wells, "The `deal.II` library, version 8.4," *Journal of Numerical Mathematics*, vol. 24, 2016.
15. C. Bruna-Rosso, A. G. Demir, B. Previtali, and M. Vedani, "Selective laser melting high performance modeling," in *Proceedings of 6th International Conference on Additive Technologies* (I. Drstvenšek, D. Drummer, and M. Schmidt, eds.), pp. 252 – 259, Interesansa - zavod, Ljubljana, 2016.
16. J. Goldak, A. Chakravarti, and M. Bibby, "A new finite element model for welding heat sources," *Metallurgical Transactions B*, vol. 15, no. 2, pp. 299–305, 1984.
17. E. R. Denlinger, V. Jagdale, G. V. Srinivasan, T. El-Wardany, and P. Michaleris, "Thermal modeling of Inconel 718 processed with powder bed fusion and experimental validation using in situ measurements," *Additive Manufacturing*, vol. 11, pp. 7 – 15, 2016.
18. L. Parry, I. A. Ashcroft, and R. D. Wildman, "Understanding the effect of laser scan strategy on residual stress in selective laser melting through thermo-mechanical simulation," *Additive Manufacturing*, vol. 12, pp. 1 – 15, 2016.
19. K. C. Mills, "Fe - 316 Stainless steel," in *Recommended Values of Thermophysical Properties for Selected Commercial Alloys*, Woodhead Publishing Series in Metals and Surface Engineering, pp. 135–142, Woodhead Publishing, 2002.
20. S. S. Sih and J. W. Barlow, "The prediction of the emissivity and thermal conductivity of powder beds," *Particulate Science and Technology*, vol. 22, no. 4, pp. 427–440, 2004.
21. J. K. Panayiotis and B. Marc-Jean, "Thermal and structural properties of fusion related materials." http://www-ferp.ucsd.edu/LIB/PROPS/PANOS/, 1997.
22. F. Pianosi, F. Sarrazin, and T. Wagener, "A Matlab toolbox for Global Sensitivity Analysis," *Environmental Modelling & Software*, vol. 70, pp. 80 – 85, 2015.
23. F. Campolongo, A. Saltelli, and J. Cariboni, "From screening to quantitative sensitivity analysis. A unified approach," *Computer Physics Communications*, vol. 182, no. 4, pp. 978 – 988, 2011.
24. P. A. Vanrolleghem, G. Mannina, A. Cosenza, and M. B. Neumann, "Global sensitivity analysis for urban water quality modelling: Terminology, convergence and comparison of different methods," *Journal of Hydrology*, vol. 522, pp. 339 – 352, 2015.
25. J. Delgado, J. Ciurana, and C. A. Rodríguez, "Influence of process parameters on part quality and mechanical properties for DMLS and SLM with iron-based materials," *The International Journal of Advanced Manufacturing Technology*, vol. 60, no. 5, pp. 601–610, 2012.
26. X. Bai, H. Zhang, and G. Wang, "Improving prediction accuracy of thermal analysis for weld-based additive manufacturing by calibrating input parameters using IR imaging," *The International Journal of Advanced Manufacturing Technology*, vol. 69, pp. 1087–1095, Nov 2013.

27. J. Romano, L. Ladani, J. Razmi, and M. Sadowski, "Temperature distribution and melt geometry in laser and electron-beam melting processes - A comparison among common materials," *Additive Manufacturing*, vol. 8, pp. 1 – 11, 2015.
28. L. Ladani, J. Romano, W. Brindley, and S. Burlatsky, "Effective liquid conductivity for improved simulation of thermal transport in laser beam melting powder bed technology," *Additive Manufacturing*, vol. 14, no. Supplement C, pp. 13 – 23, 2017.